communications earth & environment

Article

https://doi.org/10.1038/s43247-024-01404-9

Wildfire smoke reduces lake ecosystem metabolic rates unequally across a trophic gradient

Adrianne P. Smits[1] ✉, Facundo Scordo[2,6,7], Minmeng Tang[3,8], Alicia Cortés[4,5], Mary Jade Farruggia[1], Joshua Culpepper[2,9], Sudeep Chandra[2], Yufang Jin[3], Sergio A. Valbuena[4,5], Shohei Watanabe[5], Geoffrey Schladow[4,5] & Steven Sadro[1]

Wildfire smoke covers entire continents, depositing aerosols and reducing solar radiation fluxes to millions of freshwater ecosystems, yet little is known about impacts on lakes. Here, we quantified trends in the spatial extent of smoke cover in California, USA, and assessed responses of gross primary production and ecosystem respiration to smoke in 10 lakes spanning a gradient in water clarity and nutrient concentrations. From 2006 − 2022, the maximum extent of medium or high-density smoke occurring between June-October increased by 300,000 km^2. In the three smokiest years (2018, 2020, 2021), lakes experienced 23 − 45 medium or high-density smoke days, characterized by 20% lower shortwave radiation fluxes and five-fold higher atmospheric fine particulate matter concentrations. Ecosystem respiration generally declined during smoke cover, especially in low-nutrient, cold lakes, whereas responses of primary production were more variable. Lake attributes and seasonal timing of wildfires will mediate the effects of smoke on lakes.

Increasingly frequent and severe wildfires associated with climate change release vast quantities of smoke into the atmosphere[1], generating plumes that travel thousands of kilometers[2] and expose millions of water bodies to smoke for weeks to months[3]. Aerosols within smoke plumes absorb or scatter solar radiation[4], reducing total fluxes to terrestrial and aquatic ecosystems and altering the spectral composition of light. Smoke aerosol particles also contain carbon and nutrients such as phosphorus (P) and nitrogen (N), which can fertilize receiving ecosystems[5,6]. Both reduced solar radiation and particle deposition affect physical and biological processes in aquatic ecosystems, for example, by reducing water temperature[7] or altering rates of gross primary production (GPP) and ecosystem respiration (R)[8]. Changes in ecosystem metabolic rates can alter critical ecosystem processes such as carbon and nutrient cycling, rates of carbon burial and greenhouse gas emission, and food web structure[9]. Currently, little is known about how ecosystem metabolic rates may respond to wildfire smoke in lakes spanning gradients in size or productivity.

Smoke effects on ecosystem metabolic rates (i.e., GPP or R) have rarely been measured, despite the increased exposure of ecosystems to high-density smoke[3]. To date, studies of smoke impacts on ecosystems focus primarily on the effects of altered radiation fluxes to forest or cropland production[10–12], or on the effects of aerosol deposition on phytoplankton growth in oligotrophic marine systems[6,13,14]. Existing studies of smoke effects on inland waters are limited to single-site case studies (e.g., Castle Lake[8,15]; Lake Tahoe[16]) or focus on relatively few response variables (e.g., water temperature[7], cyanobacterial blooms[17]). The influence of smoke cover on freshwater ecosystems at spatial scales greater than single sites is not yet understood but is of growing importance, as wildfires release smoke across whole continents[18]. A lack of regional-scale studies limits understanding of variability in lake responses or its causes. While the influence of smoke cover on aquatic systems was first described decades ago[16], limnological research has not kept pace as wildfire smoke becomes a global rather than local phenomenon.

[1]Environmental Science and Policy, University of California Davis, Davis, CA, USA. [2]Department of Biology, University of Nevada Reno, Reno, NV, USA. [3]Land, Air, and Water Resources, University of California Davis, Davis, CA, USA. [4]Civil and Environmental Engineering, University of California Davis, Davis, CA, USA. [5]Tahoe Environmental Research Center, University of California Davis, Davis, CA, USA. [6]Present address: Instituto Argentino de Oceanografía, Universidad Nacional del Sur (UNS)-CONICET, Bahía Blanca, Buenos Aires, Argentina.[7]Present address: Departamento de Geografía y Turismo, Universidad Nacional del Sur, Bahía Blanca, Buenos Aires, Argentina.[8]Present address: Civil and Environmental Engineering, Cornell University, Ithaca, NY, USA.[9]Present address: Department of Biology, York University, Toronto, ON, Canada.. ✉e-mail: asmits@ucdavis.edu

While the effects of smoke on ecosystem rates of primary production and respiration have rarely been explored, the roles of light, temperature, and nutrients in regulating ecosystem metabolic rates have a strong theoretical underpinning and long history of empirical study[19,20]. Predicting ecosystem responses to smoke relies on understanding how the relative importance of different drivers varies across ecosystems or through time within individual systems. For example, the same reduction in photosynthetically active radiation (PAR) due to smoke might reduce rates of primary production in a eutrophic lake where phytoplankton are light-limited but increase rates of production in an oligotrophic lake with high water clarity where phytoplankton are photo-inhibited (Fig. 1a). Likewise, the effect of aerosol deposition on ecosystem metabolic rates (i.e., the fertilization effect) depends on the concentration and nutrient stoichiometry of smoke particulates[3], as well as on ambient nutrient concentrations within lakes (Fig. 1c). In contrast, reduced water temperature due to smoke cover should decrease ecosystem metabolic rates across all systems, dependent on the temperature coefficient (Q_{10}; Fig. 1b). The few existing studies of smoke effects on ecosystem metabolic rates illustrate high variability in responses in both terrestrial and aquatic systems. In a forest where smoke cover decreased total PAR fluxes, GPP was reduced at the leaf scale but increased at the canopy scale because smoke increased diffuse PAR and illuminated a greater proportion of the canopy[10]. Likewise, while GPP increased during smoke cover in surface waters within a mesotrophic lake, it declined deeper in the water column where phytoplankton were light-limited[8]. How individual ecosystems respond to smoke will consequently depend on both how smoke affects fundamental drivers (light, temperature, nutrients) and on system-specific attributes such as water clarity and nutrient concentrations.

Here we present the first regional investigation of the effects of smoke exposure on ecosystem metabolic rates in inland waters. First, we quantified annual and seasonal trends in the spatial extent of medium and high-density smoke cover (hereafter 'med-high density') in California, USA, over 18 years (2006 – 2022) using remote sensing. We then asked the following broad questions: (1) Are responses of ecosystem metabolism to smoke uniform across different types of lakes? (2) Do smoke duration, density, or seasonal timing influence how ecosystems respond?, and (3) to what extent are responses in GPP and R to smoke coupled or decoupled?

To address these questions, we quantified changes in daily shortwave radiation (SW), atmospheric fine particulate matter concentrations (PM2.5), water temperature, and ecosystem metabolism during periods of med-high density smoke cover in 9 freshwater lakes and one freshwater tidal slough in California (hereafter referred to as 'lakes'; Fig. 2a, Table 1), where wildfire extent has increased 5-fold since the 1970s[21]. We measured responses to smoke in 2018, 2020, and 2021, the three worst fire seasons on record in California[22]. We estimated rates of ecosystem metabolism from hourly dissolved oxygen (DO) measurements in both pelagic (open-water) and littoral (near-shore) environments within study sites (total = 22 datasets). Study sites spanned wide ranges in nutrient availability and water clarity, from ultra-oligotrophic (e.g., Lake Tahoe) to hyper-eutrophic (e.g., Clear Lake).

We hypothesized that ecosystem metabolic responses to smoke would vary primarily in relation to water clarity and nutrient or organic matter availability, with GPP and R tending to increase in the surface waters of oligotrophic systems but decrease in meso- or eutrophic-systems. We expected to see greater changes in metabolism during high-density, prolonged smoke cover compared to low-density or intermittent smoke events. Finally, we expected the magnitude of change in GPP and R to be coupled in oligotrophic systems, where available carbon pools are lower and respiration is primarily fueled by recent autochthonous production[23]. However, we expected GPP and R would be decoupled in more productive systems, where high organic matter and nutrient concentrations fuel respiration by heterotrophs irrespective of changes in GPP[24].

Results

Increased spatial extent and duration of medium-high density smoke in California since 2006

Averaged over the last 18 years (2006—2022), the months July, August, and September had the greatest maximum spatial extent of med-high density smoke cover in California (maximum coverage >40%; Fig. 2b), followed by June (30%) and October (18%). Two of the main study years (2020, 2021) were outliers in the seasonal timing of smoke cover: the maximum extent of med-high density smoke exceeded 70% of California in September and October in both years (Fig. 2b red points in boxplot; Supplementary Fig. 1).

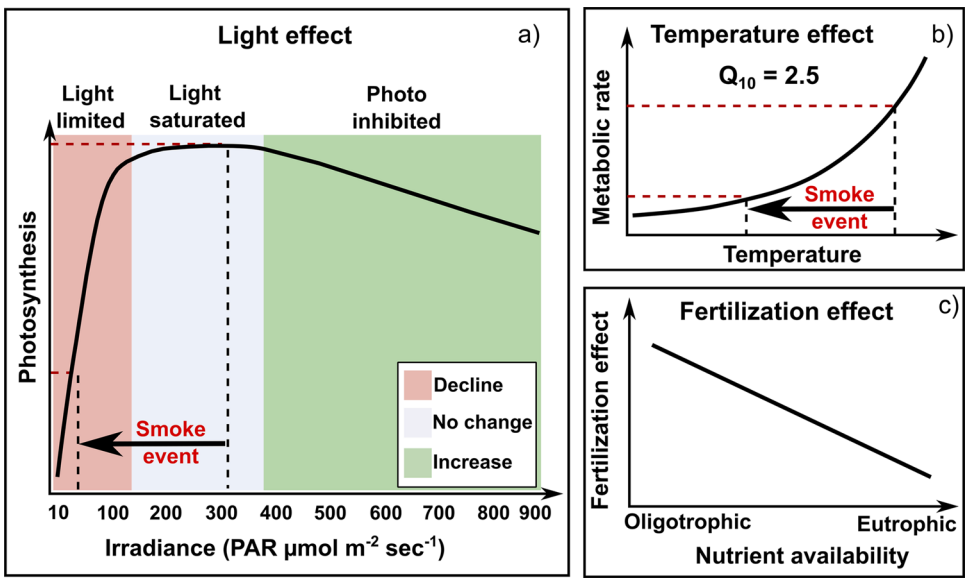

Fig. 1 | Smoke can affect aquatic ecosystem metabolism through multiple mechanisms. a Smoke events (black horizontal arrow) reduce light (PAR) within the water column. Whether a smoke event increases (green-colored region) or decreases GPP (brown-colored regions) depends on the pre-smoke PAR level and on the magnitude of PAR reduction (e.g., smoke density). In this example, a smoke event reduces GPP because primary producers shift from light-saturated to light-limited conditions. **b** Smoke events (black arrow) can reduce water temperature by scattering or absorbing incoming solar radiation, which should decrease metabolic rates (both GPP and R). **c** The degree to which nutrient fertilization from smoke particle deposition stimulates GPP depends on ambient nutrient availability within a water body.

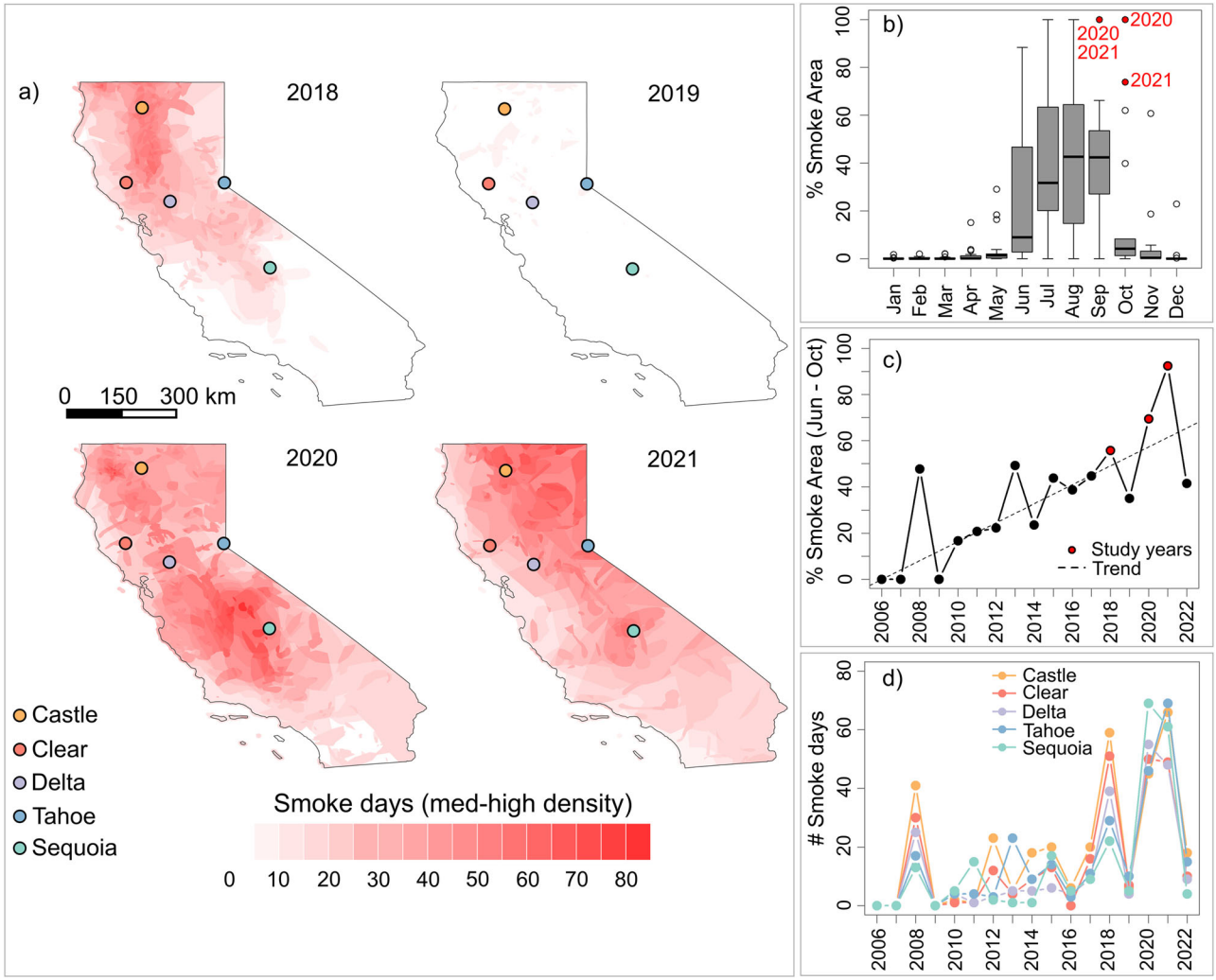

Fig. 2 | Spatial and temporal patterns in med-high density smoke cover in California (CA) and at study sites between 2006 and 2022. a Maps showing study sites (colored dots) and the annual number of days with med-high density smoke cover from 2018 to 2021 (red color gradient). Sites that are close together (ex. 5 lakes and ponds in Sequoia NP, multiple locations within the same lake) are represented by a single point. **b** Boxplots show the maximum spatial extent of med-high density smoke observed in each month (percentage of CA's area; 2006−2022). Horizontal lines in boxplots show medians, box extents show the interquartile range (IQR), whiskers extend to the greatest or smallest values within 1.5 times the IQR, and data outside this range are shown as points (outliers). Smoke cover extent in September and October of 2020 and 2021 (red labeled points) were outliers. **c** Time series of the maximum spatial extent of med-high density smoke (averaged across months June-October; points connected with solid black lines). Study years are shown as red points. The dashed line shows a significant linear trend in maximum spatial extent through time (Sen's slope). **d** Time series of the total annual days with med-high density smoke cover at study sites (points connected by solid lines, colors correspond to study sites), from 2006 to 2022. Data from study sites in close spatial proximity are not shown.

From 2006 to 2022, the maximum extent of med-high density smoke increased significantly in every month between June and October. Maximum smoke extent increased the fastest in August (23,360 km^2 $year^{-1}$ or 5.5% of California's area $year^{-1}$, Kendall's $S = 68$, $p = 0.005$, $n = 18$) and September (20,392 km^2 or 4.8% $year^{-1}$, $S = 80$, $p = 0.001$, $n = 18$), followed by July (16,704 km^2 or 3.9% $year^{-1}$, $S = 67$, $p = 0.006$, $n = 18$). Averaged across the predominant smoke season (June - October), the maximum extent of med-high density smoke cover has increased by ~300,000 km^2, or 70% of California's area, over the last 18 years ($S = 83$, $p = 0.0007$, $n = 18$; dashed line in Fig. 2c). Our study years (2018, 2020, 2021) had the greatest maximum spatial extent of med-high density smoke since 2006 (Fig. 2c).

The duration of med-high density smoke cover at the 10 study sites was highly variable among years but increased dramatically during the study years (Fig. 2d). From 2006 − 2022, sites experienced an average of 15 med-high density smoke days per year (range 0–69 days). There were regional differences in smoke duration between the study years (2018 - 2021; Fig. 2a), likely related to proximity to wildfires and prevailing wind patterns. For example, in 2021 smoke affected the northern Sierra Nevada mountains, Klamath mountains, and Sacramento Delta more than the southern Sierra Nevada mountains.

Variable lake exposure to smoke (2018, 2020, 2021)

Across all site-year combinations where independent meteorological data were available, daily mean SW radiation fluxes on smoke days were significantly less than those on non-smoke days (n = 394 smoke days, $n = 694$ non-smoke days; 205 versus 254 W m^{-2}; two-tailed $t = -11.613$, $p < 2.2 \times 10^{-16}$, df = 888.97; Fig. 3a), a reduction of 20% relative to clear-sky estimates (SW_{diff} = mean reduction 57 W m^{-2}). Atmospheric PM2.5 concentrations were elevated on smoke days compared with non-smoke days ($n = 283$ smoke days, 593 non-smoke days; 52 versus 10 μg m^{-2} $t = 12.007$, $p < 2.2 \times 10^{-16}$; Fig. 3b).

Exposure to smoke varied in duration, intermittence, and intensity across the 9 meteorological datasets (Table 2). During the three study years (2018, 2020, 2021) study sites experienced an average of 33 smoke days between July 1 and Oct 1 ($n = 9$; range 23–45 days; Table 2). The timing of smoke events varied among sites and years, but in general August and

Table 1 | Study site locations and attributes

Site name	CA region	Latitude (°)	Longitude (°)	Elevation (m.a.s.l)	Surface area (ha)	Max depth (m)	Chl-a (μg L^{-1})	PAR attenuation (k_d m^{-1})	Study period
Delta	Sacramento-San Joaquin River Delta	38.48	−121.585	0	1160	10	4.8 (3.4)	1.58	8/1/2020–11/1/2020
Clear Lake	N. Coast Range	39.064	−122.842	431	15,100	8	17.5 (9.4) LA 59.5 (38.1) OA	1.23 (0.37) LA 1.58 (0.74) OA	7/1/2020–11/1/2020; 7/1/2021–11/1/2021
Dulzura Lake (Tahoe)	N. Sierra Nevada	39.298	−120.383	2097	14.8	9.5	1.6 (1.1)	0.53 (0.03)	7/1/2021–10/1/2021
Castle Lake	Klamath	41.227	−122.383	1646	20.1	30	0.79 (0.25)	0.25 (0.01)	7/1/2018–10/1/2018
TOK 11 Pond (Sequoia)	S. Sierra Nevada	36.594	−118.671	2970	0.2	2.3	0.65 (0.60)	0.22	7/1/2020–11/1/2020; 7/1/2021–11/1/2021
EML Pond 1 (Sequoia)	S. Sierra Nevada	36.599	−118.679	2802	0.2	3.1	0.88 (0.49)	0.22	7/1/2020–11/1/2020; 7/1/2021–11/1/2021
Topaz Pond (Sequoia)	S. Sierra Nevada	36.625	−118.635	3229	0.2	1.9	0.86 (1.04)	0.22	7/1/2020–11/1/2020; 7/1/2021–11/1/2021
Topaz Lake (Sequoia)	S. Sierra Nevada	36.626	−118.637	3219	3.8	5	1.44 (0.37)	0.22	7/1/2020–11/1/2020; 7/1/2021–11/1/2021
Emerald Lake (Sequoia)	S. Sierra Nevada	36.598	−118.676	2800	2.8	10	0.74 (0.42)	0.24	7/1/2020–11/1/2020; 7/1/2021–11/1/2021
Lake Tahoe (Tahoe)	N. Sierra Nevada	39.103	−120.035	1897	49,624	501	0.31 (0.13)	0.09 (0.01)	7/1/2020–11/1/2020; 7/1/2021–11/1/2021

Names of groups of lakes corresponding to names shown in Fig. 2 are included in parentheses. For Clear Lake, data are shown for the Lower Arm (LA) and Oaks Arm (OA).

September had more smoke days than July (mean of 14 days versus 3 days), matching the results from the 18-year smoke time series (Fig. 2b). The mean length of smoke events (consecutive smoke days; $n = 87$ smoke events) ranged from 3–8 days, but there was large variation in the maximum length of smoke events across the datasets (4–21 days; Table 2). The cumulative seasonal deficit in SW fluxes due to smoke (e.g., smoke intensity; 10^6 J m^{-2}) varied three-fold among lake-years, with the greatest SW deficits at Emerald Lake (2020, 2021) and Lake Tahoe (2021) and the least at Castle Lake in 2018 (Table 2 and Fig. 3c, d).

Responses of ecosystem metabolism to smoke

Rates of ecosystem metabolism were highly variable among the 10 sites and were temporally and spatially variable within lakes (Supplementary Table 1 and Supplementary Figs. 2 and 3). Volumetric rates of GPP in pelagic habitats ranged from 0.11 ± 0.09 mg DO L^{-1} d^{-1} in oligotrophic Emerald Lake to 1.43 ± 1.26 mg DO L^{-1} d^{-1} in hyper-eutrophic Clear Lake. Littoral habitats and shallow ponds tended to have higher volumetric rates of GPP than pelagic sites or deeper lakes, ranging from 0.59 ± 0.16 mg DO L^{-1} d^{-1} in TOK 11 Pond to 1.62 ± 0.30 mg DO L^{-1} d^{-1} in Dulzura Lake. In Castle and Dulzura, where we estimated metabolism in both pelagic and littoral habitats, mean rates of GPP in littoral areas were >3 times the corresponding rates in mid-lake surface water (Supplementary Table 1). Sites with warmer water temperatures and higher chlorophyll-a (chla), total dissolved N (TDN), and total dissolved P (TDP) concentrations had higher rates of GPP (see Supplementary Table 2 for water chemistry summary; Supplementary Table 3 for correlation matrix). Respiration rates were strongly correlated with GPP overall (Pearson's $r = 0.94$, $n = 1772$ metabolism days), though the strength of this correlation varied considerably among datasets (0.34–0.96; Supplementary Table 1). R was highest in warm lakes with higher chlorophyll-a (chla) and nutrient concentrations (e.g., Delta and Clear Lake). Mean NEP was negative in 18 out of 22 datasets; only 3 littoral sites (Castle Lake, Dulzura Lake, and Lake Tahoe) and one pelagic site (Castle Lake) had positive mean NEP.

Rates of GPP (z-scored) were significantly lower on smoke days ($n = 726$) than on non-smoke days ($n = 1046$; GAMM model parametric effect of smoke = −0.22 ± 0.05 (SE), $p = 1.76 \times 10^{-5}$; Fig. 4a). Though GPP declined seasonally in the absence of smoke, smoke cover further reduced rates relative to the seasonal decline (Fig. 4d). Median GPP was lower during smoke days in most of the datasets (negative ΔGPP; Fig. 4g), decreasing by up to 70% in Clear Lake (OA) in 2020. However, median GPP was higher in certain sites and years, increasing by up to 40% in the littoral zone of Lake Tahoe in 2021 (Supplementary Fig. 3 and Supplementary Table 1). Respiration rates were lower on smoke days (smoke effect = −0.24 ± 0.05, $p = 7.02 \times 10^{-7}$, $n = 1772$, Fig. 4b), and smoke cover accelerated seasonal declines in R (Fig. 4e). Median rates of R were up to 52% lower during smoke days (EML Pond 1 in 2021). Only mesotrophic or eutrophic sites showed higher median rates of R during smoke days (positive ΔR; Fig. 4h), increasing by up to 53 % in Clear Lake (OA) in 2021. Unlike GPP and R, NEP was not significantly different between smoke and non-smoke days across all the datasets (smoke effect = 0.03 ± 0.06, $p = 0.62$; Fig. 4c, f). NEP tended to be more positive on smoke days in oligotrophic sites and more negative in mesotrophic or eutrophic sites (Fig. 4i).

Because GPP and R were coupled in most sites, responses of GPP and R to smoke (ΔGPP, ΔR) were also positively correlated (Fig. 5a; linear regression coefficient = 0.56 ± 0.16, $R^2 = 0.28$, $p = 0.003$, $n = 22$). However, no lake attribute or smoke variable explained GPP responses to smoke. ΔGPP was not related to log-TDP (Fig. 5b; $p = 0.43$), log-TDN ($p = 0.37$), log-chla ($p = 0.69$), mean summer water temperature ($p = 0.36$), or to smoke variables (Supplementary Table 3). In contrast, ΔR was positively correlated with lake variables such as mean summer water temperature (effect = 0.09 ± 0.02, $R^2 = 0.36$; $p = 0.002$), log-TDP (Fig. 5c; effect 0.19 ± 0.05, $R^2 = 0.39$, $p = 0.001$), log-TDN (effect 0.45 ± 0.13, $R^2 = 0.31$, $p = 0.003$), and log-chla (effect 0.22 ± 0.06, $R^2 = 0.37$, $p = 0.001$); respiration rates were lower on smoke days in cold, low-nutrient lakes. R was also reduced in sites that experienced more prolonged smoke cover (number of smoke days;

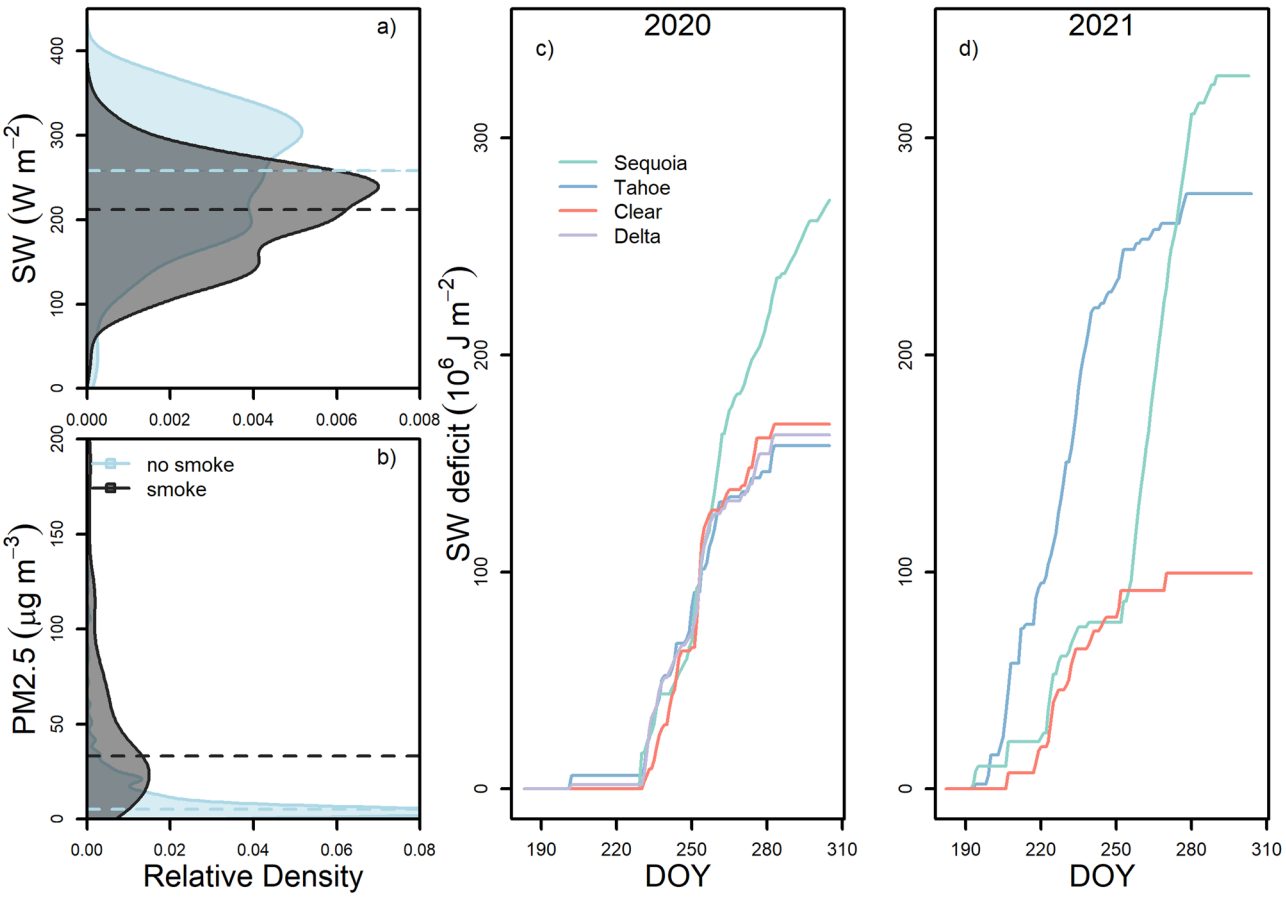

Fig. 3 | Changes in SW radiation fluxes and PM2.5 concentration during smoke cover. a Density plot of daily average SW radiation and (**b**) daily average PM2.5 concentration on non-smoke ($n = 694$; blue) and smoke ($n = 349$; gray) days. Dashed horizontal lines show median values across 9 unique meteorological datasets. **c**, **d** The cumulative deficit of SW radiation due to smoke cover (solid colored lines) from July 1 (doy 183) to Nov 1 (doy 306) in 2020 and 2021 at our study sites (line color corresponds with study site). Horizontal sections of the lines represent non-smoke days, vertical sections represent smoke events. Datasets that are spatially proximate have been omitted from panels **c**, **d**. Castle Lake's cumulative SW deficit is not shown because only data from 2018 were available. Data were not collected from the Delta site in 2021.

Table 2 | Attributes of smoke exposure for selected study sites

Site	Year	# Smoke days				# Consecutive smoke days		Mean PM2.5 (µg m^{-3})	Mean SW_{diff} (W m^{-2})	Cum. SW deficit (10^6 J m^{-2})
		Tot	Jul	Aug	Sept	Mean	Max			
Lake Tahoe	2021	45	9	23	13	3	10	51	67	260.57
Emerald Lake	2021	38	4	13	20	4	20	85	79	259.62
Emerald Lake	2020	39	0	10	28	8	21	NA	59	199.59
Dulzura Lake	2021	36	9	20	7	3	9	44	55	169.73
Clear Lake	2020	30	0	12	17	3	7	40	60	154.38
Delta	2020	34	1	13	19	4	12	47	50	145.53
Lake Tahoe	2020	28	1	12	15	3	9	28	59	143.30
Clear Lake	2021	23	1	16	6	3	5	68	50	99.35
Castle Lake	2018	26	6	12	8	3	4	34	44	97.87

Smoke attributes were calculated for the period between June 1–October 1 because some datasets were incomplete outside this date range. Mean PM2.5 and SW_{diff} refer to average values on smoke days only. Sites in close spatial proximity (e.g., small lakes and ponds in Sequoia National Park) are not shown because they lacked unique meteorological datasets.

effect = −0.04 ± 0.016, $R^2 = 0.26$, $p = 0.008$), higher smoke density (mean SW reduction on smoke days, W m^{-2}; effect = −0.03 ± 0.008, $R^2 = 0.36$, $p = 0.002$), and greater smoke intensity (cumulative SW deficit on smoke days, 10^6 J m^{-2}; effect = −0.0005 ± 0.0001, $R^2 = 0.38$, $p = 0.001$). However, because the oligotrophic lakes in the Tahoe basin and Sequoia National Park were also exposed to more prolonged and high-density smoke than the mesotrophic and eutrophic sites (Table 2 and Fig. 3c, d), we were not able to robustly distinguish the effects of smoke exposure attributes and lake variables on metabolic responses. Though littoral and pelagic habitats within the same water bodies responded differently to smoke cover, across

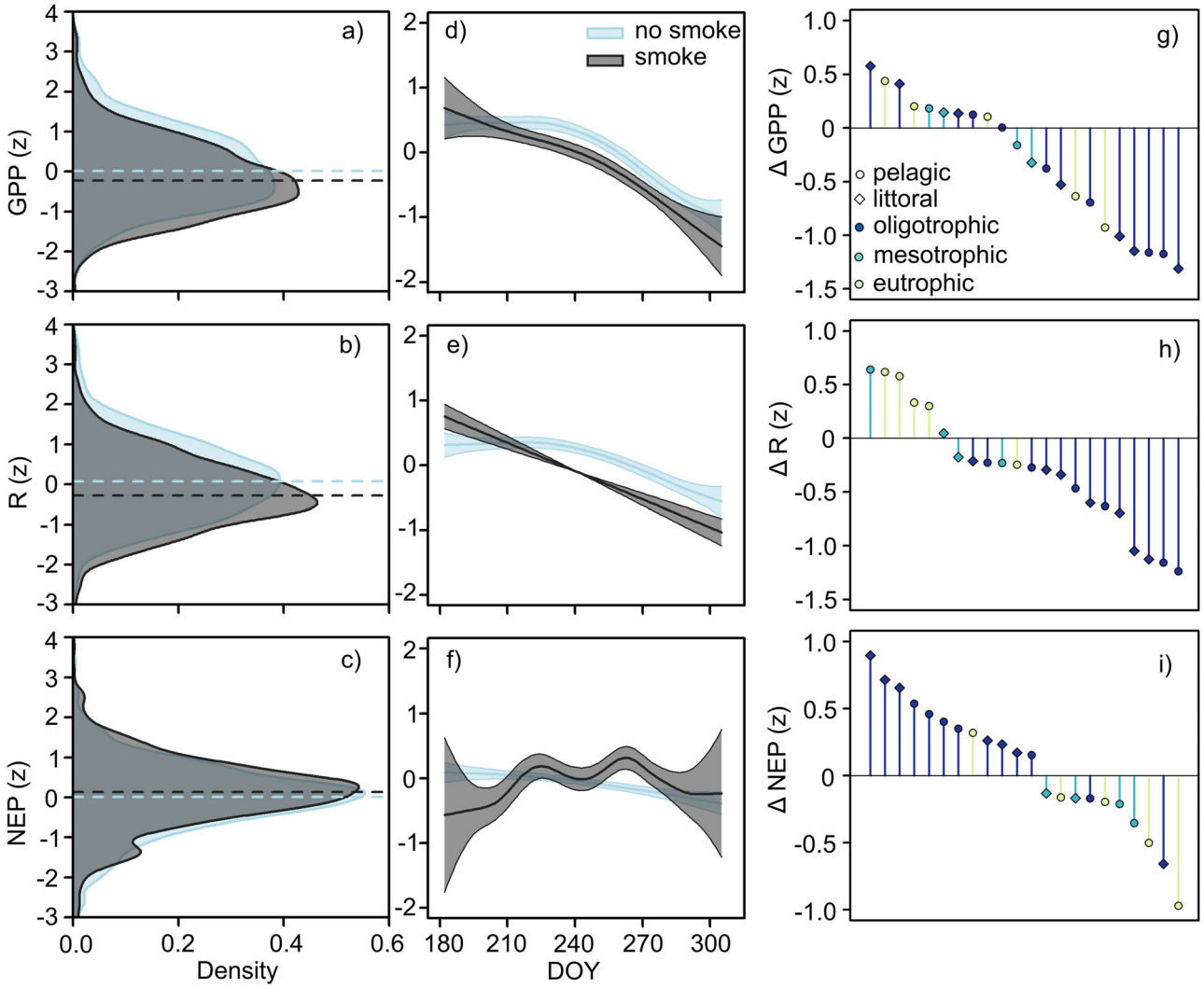

Fig. 4 | Responses of aquatic ecosystem metabolism to smoke cover. a–c Density plots of daily z-scored GPP, R, and NEP on non-smoke (blue) and smoke (gray) days ($n = 1772$). Dashed horizontal lines show the median values across all 22 metabolism datasets. **d–f** Prediction lines from the GAMM model smooth terms fit to day-of-year (gray and blue solid lines) showing how smoke cover alters seasonal trends in GPP, R, and NEP. Blue and gray shaded areas show one standard error from the predicted lines. Metabolism estimates used in GAMMs were z-scored to facilitate comparison across datasets. **g–i** The difference between median GPP, R, or NEP on smoke days versus non-smoke days (ΔGPP, R, NEP) for each dataset ($n = 22$), ordered from most positive to most negative along the x-axis. Circles represent pelagic sites; diamonds represent littoral sites. Points and segments are colored by lake trophic status (oligotrophic = blue, mesotrophic = turquoise, eutrophic = yellow-green).

sites there were no consistent differences in metabolic responses between the two habitat types.

Discussion

Overview

Our study of the impact of wildfire smoke on inland waters found highly variable responses in both GPP and R. On average, GPP and R were significantly lower on smoke days, but the magnitude and direction of responses varied considerably among and within sites. Median differences in GPP between non-smoke and smoke days ranged from +0.5 to −0.9 mg DO L^{-1} d^{-1}. Responses in R also varied but were more clearly linked to site characteristics such as nutrient concentrations and water temperature. The maximum spatial extent of med-high density smoke occurring between June-October has increased by over 50% of California's area since 2006, and smoke is associated with significant reductions in SW radiation and 4 to 5-fold increases in atmospheric PM2.5, suggesting widespread impacts to California's thousands of lakes, ponds, and tidal freshwaters[25]. These findings establish that metabolic responses of inland waters to smoke, both in the western U.S. and globally, will be highly dependent on spatial and seasonal context of smoke coverage as well as physical and chemical attributes of individual ecosystems.

Multiple mechanisms drive lake metabolic responses to wildfire smoke

We identify several potential mechanisms responsible for the variation in responses of ecosystem metabolic rates to wildfire smoke. All sites were exposed to multiple weeks of high-density smoke cover and reduced SW radiation fluxes (Table 2), yet GPP responses often differed in magnitude and direction, even within the same site, underscoring the need to better understand how changes in light affect aquatic primary producers in different habitats. In many of our datasets, GPP did not change substantially during smoky periods, suggesting that primary producers were neither strongly light-limited nor strongly photo-inhibited (Fig. 1a). Lack of strong light-limitation in our datasets is not surprising given that we only estimated GPP in the surface mixed layer—Scordo et al.[8] found that smoke cover increased GPP in surface waters but inhibited GPP in deeper waters and prevented the seasonal formation of a deep chlorophyll maximum[8]. In oligotrophic water bodies with deep chlorophyll maxima, smoke cover may

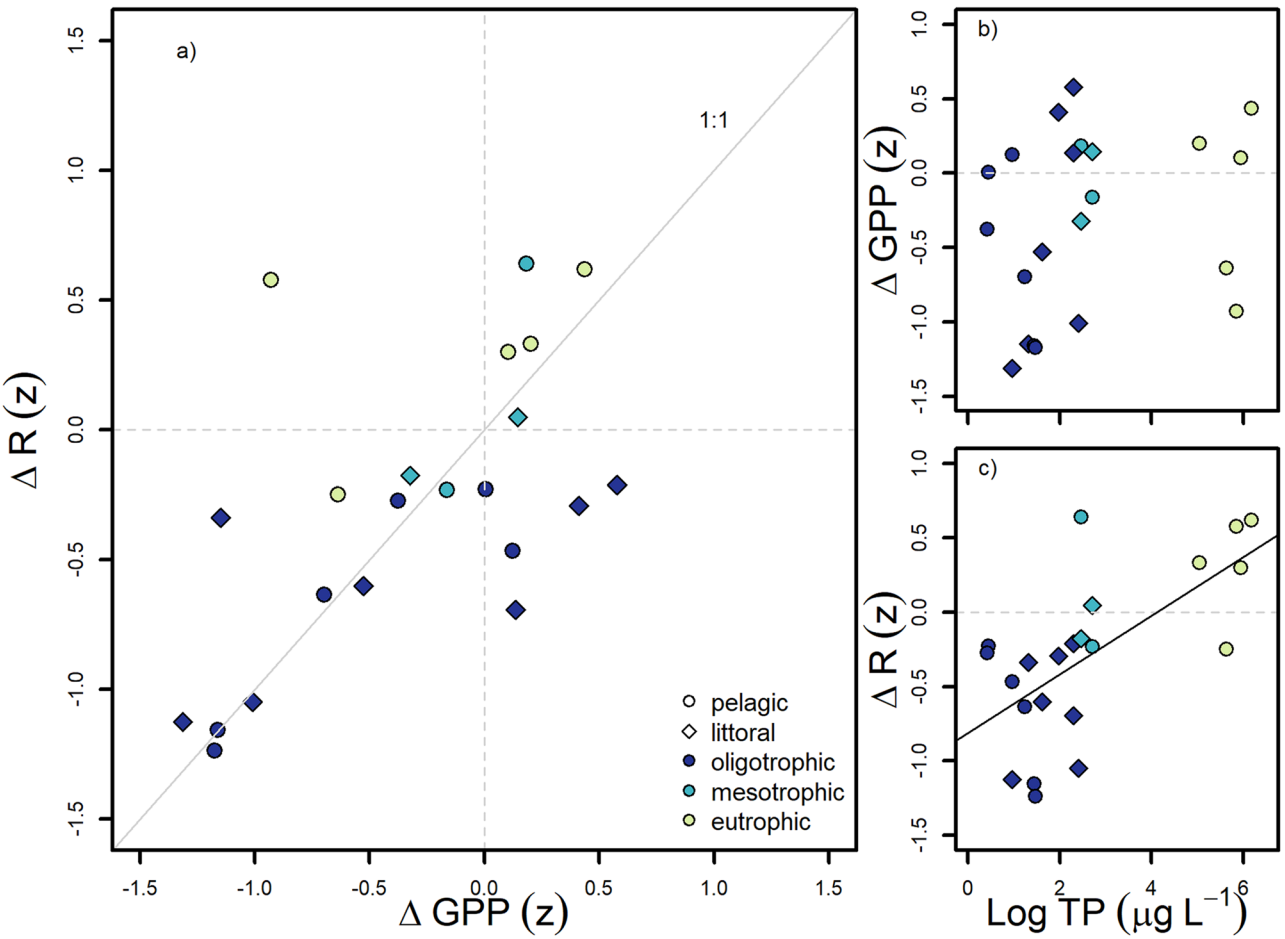

Fig. 5 | Coupling between responses of GPP and R to smoke and associations with lake nutrient concentrations. a For each dataset ($n = 22$) the median response of respiration to smoke (ΔR; z-scored; y-axis) is plotted against the median response of primary production (ΔGPP; z-scored; x-axis). Dashed horizontal and vertical lines show zero response, the gray diagonal line shows the 1:1 relationship. In all panels, circles represent pelagic sites; diamonds represent littoral sites. In all panels, points are colored by lake trophic status (oligotrophic = blue, mesotrophic = turquoise, eutrophic = yellow-green). **b** ΔGPP (z-score) plotted against mean total dissolved P (log TP; μL^{-1}). **c** ΔR (z-score) plotted against log TP. The solid black line shows a significant linear relationship ($R^2 = 0.41$, $p < 0.001$).

substantially reduce whole-lake GPP. However, we were surprised by the variable responses in littoral habitats, where we expected minimal responses due to structural and physiological adaptations by benthic algae to high-light (PAR and UV) conditions[26]. The sensitivity of aquatic primary producers to photo-inhibition has been shown to be highly taxon-specific[27], thus better characterization of algal community composition may be required to understand smoke responses in shallow or near-shore aquatic habitats.

Nutrient fertilization from smoke aerosol deposition can stimulate aquatic primary production, especially in oligotrophic systems (Fig. 1c)[6]. Phosphorus, a critical and often limiting nutrient in freshwater ecosystems, is present in significantly higher concentrations in ash compared to the unburned vegetation from which it originates[28]. However, there are few studies examining the fate of smoke particles in lakes and results are often ambiguous. Alpine lakes in proximity to biomass burning exhibited increased P concentrations and subsequently N-limitation[29]. Cyanobacterial blooms were detected via remote-sensing 2–7 days after western U.S. lakes were exposed to elevated atmospheric P concentrations from wildfire smoke smoke[17]. In ultra-oligotrophic Lake Tahoe, the addition of ash from smoke increased primary productivity relative to a control treatment, yet no significant differences were found in time series of nitrate, ammonium, or phosphate concentrations, leading the researchers to conclude that trace metals in ash, rather than N or P, increased production[16]. Scordo et al.[8] found that smoke increased particulate N and C in a mesotrophic lake, but smoke did not change the type and level of macronutrient limitation in bioassays. We did not measure nutrient concentrations at temporal resolution sufficient to test hypotheses related to nutrient fertilization, but in lakes where GPP was elevated during smoke cover, it is plausible that nutrient fertilization from particulate deposition may have stimulated primary production. However, given the importance of precipitation for mobilizing constituents from watersheds to lakes[30], it is possible that smoke exposure during California's dry summers may not lead to nutrient fertilization until the onset of autumn and winter rainstorms. Current understanding of the mechanisms and timescales of smoke-derived nutrient fertilization to lakes and their watersheds is limited[3] but an important topic for future research.

Changes in light (e.g., UV radiation) and nutrients alter ecosystem respiration rates in oligotrophic waters more so than productive waters[31]. R decreased during smoke cover in all the oligotrophic study lakes, even when GPP increased (Fig. 4g, h). Reductions in UV radiation during smoke cover should have greater effects on R in oligotrophic systems for two reasons. First, UV irradiance is higher in clear-water oligotrophic waters and imposes substantial energetic costs on aquatic organisms to repair cellular damage[32], thus UV reduction during smoke cover should decrease ecosystem respiration rates by decreasing energetic costs. Second, reducing UV improves the quality (e.g., nutrient stoichiometry) of organic matter fixed by autotrophs[33], increasing bacterial growth efficiency and decreasing ecosystem respiration rates in oligotrophic systems[34,35], where bacterioplankton account for the majority of respiration[36]. Moreover, though our study did not quantify changes in nutrient concentrations associated with ash deposition, even mild fertilization in oligotrophic surface waters can

increase C:N and C:P ratios in autotrophic biomass, increasing bacterial growth efficiency and reducing R. Impacts of prolonged smoke cover on carbon cycling and emissions from inland waters may depend equally on the responses of primary producers and heterotrophs.

Role of seasonal timing on metabolic responses to smoke

The seasonal timing of wildfire smoke cover is another important factor that can mediate lake ecosystem responses, particularly for GPP. The effects of PAR and UV reduction from smoke should vary seasonally– smoke cover in early summer, when solar radiation inputs are at their annual maximum, could stimulate GPP if phytoplankton are photo-inhibited, whereas smoke cover in autumn, when PAR is declining, may further reduce GPP (Fig. 1a). The effects of nutrient fertilization from smoke should also vary seasonally in water bodies with strong seasonal changes in nutrient limitation. For example, phytoplankton may be less nutrient-limited in autumn when mixing and thermocline deepening replenish nutrient concentrations in surface waters[37]. Two of our study years (2020, 2021) had late-season smoke cover, with high-density smoke persisting through October (Fig. 2b), which may have contributed to the overall reductions in GPP with smoke cover that we observed in our datasets. In contrast, sites where GPP increased during smoke cover (Castle Lake pelagic in 2018, Lake Tahoe littoral sites in 2021) had earlier exposure to smoke, with a greater number of smoke days in July (Table 2). Though our study took place during years with relatively late-season smoke cover, this pattern is not necessarily representative of smoke exposure in California or elsewhere. Smoke covered at least 50% of California's area during June in 7 out of 17 years (Supplementary Fig. 1). The record-breaking 2023 Canadian wildfires began in May and early June, when solar radiation fluxes were highest, and covered extensive, lake-rich regions in smoke for weeks[38]. The high degree of variation in seasonal timing of smoke cover implies that lake responses could change from year-to-year depending on the timing of wildfire ignitions.

Conclusions and opportunities

Predicting the impacts of worsening wildfire smoke on inland waters at regional to continental scales requires understanding how lake and watershed attributes mediate lake responses. In North America over a million lakes were exposed to smoke for over 30 days per year (2019-2021)[3], encompassing biomes from arctic to subtropical, and subsequently an enormous range in water temperature, clarity, and nutrient concentrations. Our study sites ranged from ultra-oligotrophic to hypereutrophic, and we observed correspondingly variable responses of lake GPP and R to smoke cover. Respiration rates responded differently in warm, eutrophic lakes than in cold, oligotrophic lakes (Figs. 4h and 5c), whereas GPP responses were not related to lake trophic status. The small, oligotrophic mountain lakes in Sequoia National Park, which are representative of a majority of California's lakes[25], experienced the greatest relative declines in R during smoke cover and often increased NEP (Supplementary Table 1 and Supplementary Fig. 3), suggesting that smoke may have regionally significant impacts on aquatic carbon cycling. In other lake regions where eutrophication or high organic matter concentrations are prevalent, smoke cover may lead to reduced NEP and greater CO_2 fluxes from lakes if GPP decreases but respiration rates remain high.

Our results highlight the need for targeted research of smoke impacts on freshwaters, as a key set of basic questions remain unresolved: (1) How do lake attributes such as water clarity, trophic status, or lake size and depth mediate metabolic responses to smoke? (2) Do the mechanistic relationships that determine responses of GPP and R to smoke cover vary among different communities of autotrophs and heterotrophs? (3) How do attributes of smoke exposure mediate lake responses?, and (4) Does prolonged, high-density smoke affect aquatic carbon cycling at regional or global scales? We were unable to clearly distinguish the roles of smoke exposure attributes and lake attributes in mediating metabolic responses to smoke, due to covariation in these factors and the limited number of datasets in our study. Understanding lake responses to smoke will require extensive data collection across different hydroclimatic conditions, environmental gradients (geomorphology, vegetation, land use), and gradients in smoke exposure. Additional experimental, empirical, and modeling studies are also needed to understand the predominant mechanisms underlying whole-ecosystem metabolic responses to smoke. Even small impacts on ecosystem metabolic rates may have important implications for global carbon cycling given the large number of lakes affected by smoke globally[3]. Quantifying impacts of smoke on aquatic carbon cycling at regional to continental scales will require collaborative research within and across regions. Global-scale, opportunistic data collection by lake sensor networks such as the Global Lake Ecological Observatory Network (GLEON; https://gleon.org/) could be used to test hypotheses and broaden our understanding of this increasing global phenomenon, as wildfires and smoke cover increase in frequency, intensity, and spatial extent.

Methods

Study sites and in-situ data collection

We collected continuous hourly DO and water temperature data from 10 water bodies distributed across the northern two-thirds of California, USA, from June to October in 2018, 2020, and 2021 (Table 1 and Fig. 2). Study sites are located in several of the major mountain ranges in California, including the southern Sierra Nevada (5 sites; 'Sequoia lakes'), northern Sierra Nevada (2 sites; Lake Tahoe and Dulzura Lake; 'Tahoe lakes'), Klamath Mountains (1 site; Castle Lake), and northern Coast Range mountains (1 site; Clear Lake), as well as within the Sacramento-San Joaquin River Delta (1 site; Delta). Sites were selected to represent a large gradient in water clarity (k_d 0.09 – 1.58 m^{-1}) and lake trophic status (ultra-oligotrophic - hypereutrophic; Table 1). Sites also varied substantially in elevation (0–3200 m.a.s.l) and size (0.2–49624 ha).

Water bodies were instrumented with continuous in situ DO and temperature sensors at 1-2 locations per site (14 total sensor locations). In 7 sites (Sequoia lakes, Clear Lake, and Delta), DO and temperature were measured only in pelagic (mid-lake) habitats. In two lakes (Castle, Dulzura), DO and temperature were measured in both pelagic and littoral habitats. In Lake Tahoe, DO and temperature were only measured in two littoral sites. For all lakes, DO and temperature data were only available for a subset of the three study years (Table 1). In addition to hourly sensor data, for each lake and year we obtained water chemistry data collected from lake surface waters (0- 3 m depth) between June 1 and November 1, for the following constituents: chlorophyll-a concentration (chla; $\mu g\ L^{-1}$), total dissolved phosphorus (TDP; $\mu g\ L^{-1}$), and total dissolved nitrogen (TDN; $\mu g\ L^{-1}$). Water chemistry data were used to classify lake trophic status but were not collected at sufficient temporal resolution to evaluate changes associated with particulate deposition from smoke. Vertical profiles for photosynthetically active radiation (PAR) were collected 1–11 times per season in each lake to estimate attenuation coefficients (k_d).

Meteorological data corresponding to time periods of in-situ sensor data collection were obtained for each lake from the nearest available weather station (SW radiation, W m^{-2}; wind speed, m s^{-1}; air temperature, °C). We also obtained mean daily atmospheric fine particulate matter concentrations (<2.5 μm in diameter; PM2.5; $\mu g\ m^{-2}$) from the nearest PurpleAir or EPA sensor. PM2.5 concentrations from PurpleAir sensors were adjusted using the linear correction in Barkjohn et al.[39] to account for bias. No PM2.5 data are available for the Sequoia Lakes in 2020. In total, we compiled 22 hourly DO and water temperature datasets, 9 corresponding hourly meteorological datasets, 8 daily PM2.5 datasets, and 19 water chemistry datasets. Detailed site and dataset descriptions can be found in Supplementary Methods.

Quantifying patterns and trends in California smoke cover

We used the smoke plume product from the NOAA/NESDIS Satellite Analysis Branch's Hazard Mapping System (HMS)[40], to quantify the spatial and temporal patterns of smoke cover in California from 2006 to 2022. This product provides a daily smoke plume density polygon over North America at a 4 km resolution by integrating near real-time polar-orbiting and geostationary satellite imagery from Geostationary Operational

Environmental Satellite Program (GOES), Moderate Resolution Imaging Spectroradiometer (MODIS), and Advanced Very High Resolution Radiometer (AVHRR). This remote sensing product classified smoke plumes into three categories: low, medium, and high density, based on the estimated smoke concentrations of 5, 16, and 27 μg m^{-3}, respectively.

To quantify the spatial extent and duration of smoke cover in California for each year, we made an annual composite map of smoke cover by intersecting daily smoke plume polygons with each intersecting polygon recording the number of smoke days for a given year. All areas exposed to smoke for at least one day were then summarized to quantify the annual spatial extent of smoke cover. This process was repeated for each month to evaluate the seasonal and interannual patterns of smoke cover extent in California, for each smoke density. In further analyses, we focused on medium and high-density smoke cover (hereafter 'med-high density') rather than low density smoke cover because we assumed more dense smoke cover would be of greater ecological relevance (e.g., more likely to reduce SW radiation fluxes and deposit particulates into lakes).

We assessed time series of the maximum extent of med-high density smoke cover in the months June-October, as well as annual and seasonal means, for monotonic trends by computing Sen's slopes and applying the Mann-Kendall test using the 'wql' package in R[41].

In addition to quantifying smoke cover throughout California, we generated a daily smoke density sequence over each study lake from 2006 – 2022. First, we obtained lake shapefiles from the California Lake database maintained by California Department of Fish and Wildlife (CDFW)[42]. For study sites that were not included in the California Lake database (e.g., small ponds in Sequoia National Park), we used a 100 meter buffer around the central point in the lake as an approximation of the lake surface. We then assigned a daily smoke density value to each lake by comparing spatial relationships between smoke plume polygons and lake surfaces. If a smoke plume intersected a lake's surface area, we assigned the corresponding smoke density to the lake based on the date. If multiple smoke densities were assigned to the same lake on the same date, only the highest smoke density was assigned.

Characterizing lake exposure to smoke during study period

We identified periods of smoke cover for each lake during the study years (2018, 2020, 2021) using a combination of the daily smoke density value (described in previous section), SW radiation measurements from local weather stations, PM2.5 concentrations, and visual inspection of Sentinel satellite images to confirm the presence of smoke plumes.

At each lake, we used both the remote sensing-derived smoke density values and local meteorological data to conservatively classify each day as 'smoke' or 'non-smoke'. We modeled theoretical 'clear-sky' SW radiation ($SW_{clear.sky}$) for each day using a statistical clear sky algorithm[43]. We then subtracted the measured daily mean SW (SW_{meas}) from $SW_{clear.sky}$ ($SW_{diff} = SW_{clear.sky} - SW_{meas}$). We calculated the median value of SW_{diff} on days with smoke density of zero across all 9 meteorological datasets (median SW_{diff} = 20 W m^{-2}). Days were then classified as smoke days if they met two conditions: (1) daily mean SW radiation was reduced by more than 20 W m^{-2}, and (2) smoke density was medium or high.

For each lake-year combination, we characterized the following attributes of smoke exposure: (1) the total number of smoke days between July 1-Oct 1; (2) the intermittence of smoke cover, defined as the mean, median, and maximum number of consecutive smoke days that occurred in each dataset; and (3) the cumulative reduction in SW radiation relative to clear sky values on smoke days ('cumulative SW deficit'). We calculated cumulative SW deficit by summing SW_{diff} on all smoke days between July 1 and October 1. Attributes of smoke cover were only quantified between July 1 - October 1 because some datasets were incomplete outside this seasonal window.

Estimating aquatic ecosystem metabolic rates

We modeled daily rates of gross primary production (GPP; mg DO L^{-1} d^{-1}), ecosystem respiration (R), and net ecosystem production (NEP = GPP - R) in the surface mixed layer of our study sites using hourly DO (mg L^{-1}), water temperature (° C), SW radiation (W m^{-2}), and wind speed (m s^{-1}) data using the Lake Metabolizer R package[44]. The metabolism models in Lake Metabolizer have been used in diverse lake types (ex. arctic, alpine[45], forested, agricultural[46]), and are described in detail in Winslow et al.[44]. A metabolism model was fitted to each DO time series using the following equation:

$$DO_{t+1} = DO_t + GPP - R + F + \varepsilon \quad (1)$$

F is the flux of oxygen between the lake and atmosphere, and ε is the process error associated with vertical or horizontal mixing. We used the 'metab' function and bayesian model to estimate daily parameters for GPP and R as well as associated uncertainty in each estimate (expressed as a standard deviation; reported in Supplementary Table 1). In the bayesian model, PAR (μmol m^{-2} s^{-1}) and water temperature are covariates used to model rates of GPP and R, respectively. In addition to hourly DO, water temperature, SW radiation, and wind speed, the following model inputs were used: depth of the surface mixed layer at each time step (z_{mix}; m), the attenuation coefficient for PAR (k_d; m^{-1}), and lake surface area (m^2).

For pelagic sites in lakes that stratified seasonally or periodically (Emerald Lake, Topaz Lake, Castle Lake, Clear Lake) we estimated metabolic rates in the surface mixed layer. We calculated mixed layer depth (Z_{mix}) using depth-distributed water temperature measurements from fixed depth sensors or vertical profiles using LakeAnalyzer in R[47]. For littoral sites within stratified lakes (Castle Lake, Dulzura Lake, Lake Tahoe), and in small, shallow water bodies that did not stratify (TOK 11 Pond, EML Pond 1, Topaz Pond), Z_{mix} was set to lake depth at the location of the DO sensor. In the tidally-influenced Delta, Z_{mix} was set to the mean depth of the channel within the range of the tidal excursion.

To estimate oxygen fluxes across the air-water interface (F), we used a wind-based gas exchange model that accounted for lake surface area[48]. We set gas exchange to zero during periods when the DO sensor was below the diel or seasonal thermocline. We estimated average PAR within the surface mixed layer by converting shortwave radiation measurements from weather stations to surface PAR and then using the attenuation coefficient for PAR (k_d; m^{-1}; Table 1; Supplementary Fig. 4) and Z_{mix} to estimate mean water column PAR as in Staehr et al.[49]. Days with unrealistic metabolism estimates (negative GPP, positive R) were excluded from results. Additional details on datasets and metabolism models can be found in the Supplementary Methods.

Quantifying effects of smoke cover on ecosystem metabolic rates

We quantified ecosystem metabolic responses to smoke cover (e.g., compared GPP, R, and NEP between smoke and non-smoke days) by fitting generalized additive mixed models (GAMMs) to the daily metabolism estimates using the 'mgcv' R package[50]. We combined the datasets to fit a single GAMM each for GPP, R, and NEP. To facilitate comparisons across sites spanning from hyper-eutrophic (Clear Lake) to ultra-oligotrophic (Lake Tahoe), we standardized metabolism time series by mean and variance (z-score) before combining datasets. We modeled daily metabolic estimates as a function of smoke cover (categorical: smoke or non-smoke) and day of year (doy; smooth term). We included an interaction between doy and smoke (e.g., estimated separate seasonal smooths terms for non-smoke and smoke days) to visualize the effect of smoke cover on seasonal patterns in metabolism. We included a random effect for site in each model to account for the non-independence of repeated measurements in each lake. As an example using R pseudocode, the model formulation for GPP is: GPP ~ re(site) + smoke + s(DOY, by = smoke), where re() is a random effect, smoke is a parametric term, and s() indicates a smooth term with an interaction. We used default thin plate regression splines for the smooth terms. GAMMs were fitted using restricted maximum likelihood estimation.

To quantify how lake and smoke attributes mediated metabolic responses to smoke cover, we calculated the median difference in

standardized metabolic rates between smoke and non-smoke days for each dataset ('metabolic response'; ΔGPP, ΔR), and then fitted linear regressions between metabolic responses and lake or smoke variables. Lake variables included log-TDN, log-TDP, log-chla, and mean summer water temperature. Smoke variables included the total number of smoke days (duration), the mean SW reduction on smoke days (metric of smoke density; W m^{-2}) and the cumulative SW reduction on smoke days (10^6 J m^{-2}), a metric of smoke intensity that incorporates both duration and density.

Reporting summary

Further information on research design is available in the Nature Portfolio Reporting Summary linked to this article.

Data availability

Daily metabolic rate estimates, meteorological data, and smoke data are available on the Environmental Data Initiative repository (https://doi.org/10.6073/pasta/440f79a43d9b23229daf0cb33a295c5d)[51].

Code availability

All code used in this paper is available from published packages cited in the references.

Received: 6 December 2023; Accepted: 19 April 2024;
Published online: 22 May 2024

References

1. Senande-Rivera, M., Insua-Costa, D. & Miguez-Macho, G. Spatial and temporal expansion of global wildland fire activity in response to climate change. *Nat. Commun.* **13**, 1208 (2022).
2. Baars, H. et al. Californian wildfire smoke over Europe: a first example of the aerosol observing capabilities of aeolus compared to ground-based lidar. *Geophys. Res. Lett*. **48**, 8 (2021).
3. Farruggia, M. J. et al. Wildfire smoke impacts lake ecosystems. *EarthArXiv*. https://doi.org/10.31223/X53H41 (2023).
4. McLauchlan, K. K. et al. Fire as a fundamental ecological process: research advances and frontiers. *J. Ecol.* **108**, 2047–2069 (2020).
5. Vicars, W. C., Sickman, J. O. & Ziemann, P. J. Atmospheric phosphorus deposition at a montane site: Size distribution, effects of wildfire, and ecological implications. *Atmos. Environ.* **44**, 2813–2821 (2010).
6. Tang, W. et al. Widespread phytoplankton blooms triggered by 2019–2020 Australian wildfires. *Nature* **597**, 370–375 (2021).
7. David, A. T., Asarian, J. E. & Lake, F. K. Wildfire smoke cools summer river and stream water temperatures. *Water Resour. Res.* **54**, 7273–7290 (2018).
8. Scordo, F. et al. Smoke from regional wildfires alters lake ecology. *Sci. Rep.* **11**, 1–14 (2021).
9. Allen, A. P., Gillooly, J. F. & Brown, J. H. Linking the global carbon cycle to individual metabolism. *Funct. Ecol.* **19**, 202–213 (2005).
10. Rastogi, B. et al. Enhanced photosynthesis and transpiration in an old growth forest due to wildfire smoke. *Geophys. Res. Lett.* **49**, 1–13 (2022).
11. Corwin, K. A., Corr, C. A., Burkhardt, J. & Fischer, E. V. Smoke-driven changes in photosynthetically active radiation during the U.S. Agricultural Growing Season. *J. Geophys. Res. Atmos*. **127**, https://doi.org/10.1029/2022JD037446 (2022).
12. Hemes, K. S., Verfaillie, J. & Baldocchi, D. D. Wildfire-Smoke aerosols lead to increased light use efficiency among agricultural and restored wetland land uses in California's central valley. *J. Geophys. Res. Biogeosci.* **125**, 1–21 (2020).
13. Ardyna, M. et al. Wildfire aerosol deposition likely amplified a summertime Arctic phytoplankton bloom. *Commun. Earth Environ.* **3**, 1–8 (2022).
14. Li, M., Shen, F. & Sun, X. 2019–2020 Australian bushfire air particulate pollution and impact on the South Pacific Ocean. *Sci. Rep.* **11**, 1–13 (2021).
15. Scordo, F., Sadro, S., Culpepper, J., Seitz, C. & Chandra, S. Wildfire smoke effects on lake-habitat specific metabolism: toward a conceptual understanding. *Geophys. Res. Lett.* **49**, 1–10 (2022).
16. Goldman, C. R., Jassby, A. D. & de Amezaga, E. Forest fires, atmospheric deposition and primary productivity at Lake Tahoe, California-Nevada. *Int. Vereinigung für Theor. und Angew. Limnol. Verhandlungen* **24**, 499–503 (1990).
17. Olson, N. E., Boaggio, K. L., Rice, R. B., Foley, K. M. & LeDuc, S. D. Wildfires in the western United States are mobilizing PM2.5-associated nutrients and may be contributing to downwind cyanobacteria blooms. *Environ. Sci.: Process. Impacts* **25**, 1049–1066 (2023).
18. Junghenn Noyes, K. T., Kahn, R. A., Limbacher, J. A. & Li, Z. Canadian and Alaskan wildfire smoke particle properties, their evolution, and controlling factors, from satellite observations. *Atmos. Chem. Phys.* **22**, 10267–10290 (2022).
19. Staehr, P. A. et al. The metabolism of aquatic ecosystems: history, applications, and future challenges. *Aquat. Sci.* **74**, 15–29 (2012).
20. Kanniah, K. D., Beringer, J., North, P. & Hutley, L. Control of atmospheric particles on diffuse radiation and terrestrial plant productivity: a review. *Prog. Phys. Geogr.* **36**, 209–237 (2012).
21. Williams, A. P. et al. Observed impacts of anthropogenic climate change on wildfire in California. *Earth's Future* **7**, 892–910 (2019).
22. Cal Fire Incidents. Available at https://www.fire.ca.gov/incidents. (2023) (Accessed: 1st July 2023).
23. Solomon, C. T. et al. Ecosystem respiration: drivers of daily variability and background respiration in lakes around the globe. *Limnol. Oceanogr.* **58**, 849–866 (2013).
24. Smith, E. M. & Prairie, Y. T. Bacterial metabolism and growth efficiency in lakes: the importance of phosphorus availability. *Limnol. Oceanogr.* **49**, 137–147 (2004).
25. Melack, J. M., Sadro, S., Sickman, J. O. & Dozier., J. *Lakes and watersheds in the Sierra Nevada of California: Responses to environmental change*. (Univ. Calif. Press., 2021).
26. Vinebrooke, R. D. & Leavitt, P. R. Differential responses of littoral communities to ultraviolet radiation in an alpine lake. *Ecology* **80**, 223 (1999).
27. Vincent, W. F. & Roy, S. Solar ultraviolet-B radiation and aquatic primary production: damage, protection, and recovery. *Environ. Rev.* **1**, 1–12 (1993).
28. Raison, R. J., Khanna, P. K. & Woods, P. V. Transfer of elements to the atmosphere during low-intensity prescribed fires in three Australian subalpine eucalypt forests. *Can. J. For. Res.* **15**, 657–664 (1985).
29. Brahney, J., Mahowald, N., Ward, D. S., Ballantyne, A. P. & Neff, J. C. Is atmospheric phosphorus pollution altering global alpine lake stoichiometry? *Glob. Biogeochem. Cycles* 1369–1383 https://doi.org/10.1002/2015GB005137 (2015).
30. Sadro, S. & Melack, J. The effect of an extreme rain event on the biogeochemistry and ecosystem metabolism of an oligotrophic high-elevation lake. *Arctic Antarct. Alp. Res.* **44**, 222–231 (2012).
31. Roberts, B. J. & Howarth, R. W. Nutrient and light availability regulate the relative contribution of autotrophs and heterotrophs to respiration in freshwater pelagic ecosystems. *Limnol. Oceanogr.* **51**, 288–298 (2006).
32. Zagarese, H. E. & Craig, E. W. Impact of solar UV radiation on zooplankton and fish. *The effects of UV radiation in the marine environment*. (eds. De Mora, S., Demers, S. & Vernet, M.) 279 (Cambridge University Press, 2000).
33. Harrison, J. W. & Smith, R. E. H. Effects of ultraviolet radiation on the productivity and composition of freshwater phytoplankton communities. *Photochem. Photobiol. Sci.* **8**, 1218–1232 (2009).
34. Tranvik, L. J. & Bertilsson, S. Contrasting effects of solar UV radiation on dissolved organic sources for bacterial growth. *Ecol. Lett.* **4**, 458–463 (2001).
35. Sadro, S., Nelson, C. E. & Melacka, J. M. Linking diel patterns in community respiration to bacterioplankton in an oligotrophic high-elevation lake. *Limnol. Oceanogr.* **56**, 540–550 (2011).

36. Biddanda, B., Ogdahl, M. & Cotner, J. Dominance of bacterial metabolism in oligotrophic relative to eutrophic waters. *Limnol. Oceanogr.* **46**, 730–739 (2001).
37. Sadro, S., Melack, J. M. & MacIntyre, S. Depth-integrated estimates of ecosystem metabolism in a high-elevation lake (Emerald Lake, Sierra Nevada, California). *Limnol. Oceanogr.* **56**, 1764–1780 (2011).
38. Dong, M. et al. *Maps: Tracking Air Quality and Smoke From Wildfires*. Available at: https://www.nytimes.com/interactive/2023/us/smoke-maps-canada-fires.html?searchResultPosition=14 (2023).
39. Barkjohn, K. K., Gantt, B. & Clements, A. L. Development and application of a United States wide correction for PM2.5 data collected with the PurpleAir sensor. *Atmos. Meas. Technol.* **4**, 4617–4637 (2021).
40. Hazard Mapping System Fire and Smoke Product Available at: https://www.ospo.noaa.gov/Products/land/hms.html#stats-smoke. (2023) (Accessed: 1st July 2023).
41. Jassby, A. D. & Cloern, J. E. *wq: Exploring Water Quality Monitoring Data* (2022).
42. California Department of Fish and Wildlife. *California Lake Database*. Available at: https://data-cdfw.opendata.arcgis.com/datasets/CDFW::california-lakes (2022).
43. Meyers, B., Tabone, M. & Kara, E. C. Statistical clear sky fitting algorithm. *arXiv* https://doi.org/10.48550/arXiv.1907.08279 (2019).
44. Winslow, L. A. et al. LakeMetabolizer: an R package for estimating lake metabolism from free-water oxygen using diverse statistical models. *Inl. Waters* **6**, 622–636 (2016).
45. Klaus, M., Verheijen, H. A., Karlsson, J. & Seekell, D. A. Depth and basin shape constrain ecosystem metabolism in lakes dominated by benthic primary producers. *Limnol. Oceanogr.* **67**, 2763–2778 (2022).
46. Corman, J. R. et al. Response of lake metabolism to catchment inputs inferred using high-frequency lake and stream data from across the northern hemisphere. *Limnol. Oceanogr.* **68**, 2617–2631 (2023).
47. Read, J. S. et al. Derivation of lake mixing and stratification indices from high-resolution lake buoy data. *Environ. Model. Softw.* **26**, 1325–1336 (2011).
48. Vachon, D. & Prairie, Y. T. The ecosystem size and shape dependence of gas transfer velocity versus wind speed relationships in lakes. *Can. J. Fish. Aquat. Sci.* **70**, 1757–1764 (2013).
49. Staehr, P. A., Brighenti, L. S., Honti, M., Christensen, J. & Rose, K. C. Global patterns of light saturation and photoinhibition of lake primary production. *Inl. Waters* **6**, 593–607 (2016).
50. Wood, S. N. Fast stable restricted maximum likelihood and marginal likelihood estimation of semiparametric generalized linear models. *J. R. Stat. Soc. Ser. B Stat. Methodol.* **73**, 3–36 (2011).
51. Smits, A. P. et al. Study of wildfire smoke effects on ecosystem metabolism in 10 California lakes (2018, 2020, 2021) ver 1. *Environmental Data Initiative*. https://doi.org/10.6073/pasta/440f79a43d9b23229daf0cb33a295c5d (2024).

Acknowledgements

A.P.S. and A.C. were supported by NSF RAPID Award # 2102344 to S.S., Y.J., and G.S.; M.J.F. was supported by NSF GRFP Award # 2036201. S.A.V. and S.W. were supported by the Tahoe Regional Planning Agency and the Lahontan Regional Water Quality Control Board. U.S. Bureau of Reclamation award #R21AC10519-00 to SS.

Author contributions

A.P.S. designed the study, provided datasets, performed data analyses, made figures, and led manuscript writing. F.S. designed the study, provided datasets, performed data analyses, made figures, and helped write the manuscript. M.T. provided datasets, performed data analyses, made figures, and helped write the manuscript. A.C. provided datasets, performed data analyses, and helped write the manuscript. M.J.F. provided datasets, performed data analyses, and helped write the manuscript. J.C. provided datasets, performed data analyses, and helped write the manuscript. S.C. provided datasets and helped write the manuscript. Y.J. interpreted data and helped write the manuscript. S.A.V. provided datasets and helped write the manuscript. S.W. provided datasets and helped write the manuscript. G.S. interpreted data and helped write the manuscript. S.S. designed the study, provided datasets, made figures, and helped write the manuscript.

Competing interests

The authors declare no competing interests.

Additional information

Supplementary information The online version contains supplementary material available at https://doi.org/10.1038/s43247-024-01404-9.

Correspondence and requests for materials should be addressed to Adrianne P. Smits.

Peer review information *Communications Earth and Environment* thanks Onja Raoelison and the other, anonymous, reviewer(s) for their contribution to the peer review of this work. Primary Handling Editors: Mengze Li, Joe Aslin and Clare Davis. A peer review file is available.